MAX-PLANCK-INSTITUT FÜR PLASMAPHYSIK

GARCHING BEI MÜNCHEN

Calculation of free-free radiation from plasmas with non-Maxwellian isotropic or anisotropic electron velocity distribution

K. Eidmann

IPP IV/58 July 1973

Die nachstehende Arbeit wurde im Rahmen des Vertrages zwischen dem Max-Planck-Institut für Plasmaphysik und der Europäischen Atomgemeinschaft über die Zusammenarbeit auf dem Gebiete der Plasmaphysik durchgeführt.

IPP IV/58 K. Eidmann

Calculation of free-free radiation from plasmas with non-Maxwellian isotropic or anisotropic electron velocity distribution

July 1973 (in English)

Abstract

Calculations of the bremsstrahlung resulting from electron ion collisions in plasmas with non-Maxwellian electron velocity distributions are made with special regard to laser produced plasmas. The quantum mechanical theory has been used with restriction to non-relativistic electron energies and a pure Coulomb potential of the ions within the plasma. Results for the spectrum, the angular dependence, the intensity and the polarization of the emitted bremsstrahlung for some examples of non-Maxwellian isotropic and anisotropic electron velocity distributions are presented.

1. Introduction

The emission of free-free radiation due to electron ion collisions in a plasma with an isotropic Maxwellian electron velocity distribution has been studied by many authors; see, for example, /1/. However, since plasmas are often very far from thermal equilibrium, situations with non-Maxwellian electron velocity distributions are possible, thus giving rise to bremsstrahlung emission which deviates from the Maxwellian case.

An example is the plasma produced by very high power lasers /2/, which is of interest for fusion based on the principle of inertial confinement /3/. Theory predicts, that at hight laser intensities fast electrons can be created in this plasma owing to numerous collisionless light absorption mechanisms /4/. If these mechanisms give rise to an anisotropic velocity distribution, the x-rays are emitted anisotropically.

Measurements of the x-ray emission from laser produced plasmas show non-Maxwellian bremsstrahlung spectra with an excess of energetic x-rays for photon energies exceeding a few keV up to loo keV, which can be explained by an excess of fast electrons /5, 6/. In addition, first attempts were undertaken to measure the angular dependence of the intensity and polarization of the energetic x-rays /6, 7/. Weak polarization of the x-rays emitted from ps-laser produced plasmas was observed /7/, whereas in the case of a ns-laser produced plasma isotropic emission of the intensity was measured /6/.

In this paper calculations of the x-ray emission from plasmas with non-Maxwellian isotropic as well as anisotropic electron velocity distributions with special regard to laser produced plasmas are presented. Similar calculations for the special case of a mirror confined plasma were made in /8/.

2. Calculation of free-free radiation

If an electron of kinetic energy $E_1 = \frac{m}{2} v_1^2$ collides with an ion at rest of charge Ze a photon of energy $h\nu$ is emitted. As the classical treatment of this process gives incorrect results, especially at the short wave limit, and as an essential contribution of the radiation emitted from a plasma stems from the short wave limit, a quantum mechanical calculation is necessary. Here we restrict ourselves to electron energies not exceeding about 5o keV. For this non-relativistic case Sommerfeld solved the problem using quantum mechanics exactly for a pure Coulomb potential of the ions /9/. According to this theory, for an electron incident along the x-axis the intensity I ("energy per unit solid angle per unit frequency of the emitted photon per bombarding electron per ion per unit target area") and the polarization P defined by $P = (\tilde{I} - I_y)/(\tilde{I} + I_y)$, see fig.1, are given by

$$I(\vartheta) = I_x \sin^2\vartheta + I_y (1 + \cos^2\vartheta) \tag{1}$$

and

$$P(\vartheta) = (I_x - I_y)\Big/\left(I_x + I_y \frac{\cos^2\vartheta + 1}{\sin^2\vartheta}\right) \tag{2}$$

ϑ is the angle of observation (see fig.1), I_x and I_y are functions of the two parameters E_1/Z^2 and $h\nu/E_1$. I_x and I_y involve integration over all angles of the outgoing electron wave (corresponding classically to integration over the collision parameters) and can be represented in the form /1o/:

$$I_{x,y} = (1 - \exp(-2\pi i n_2))^{-1} \cdot (\exp(2\pi i n_1) - 1)^{-1} \cdot D \cdot \mathfrak{M}_{x,y} \tag{3}$$

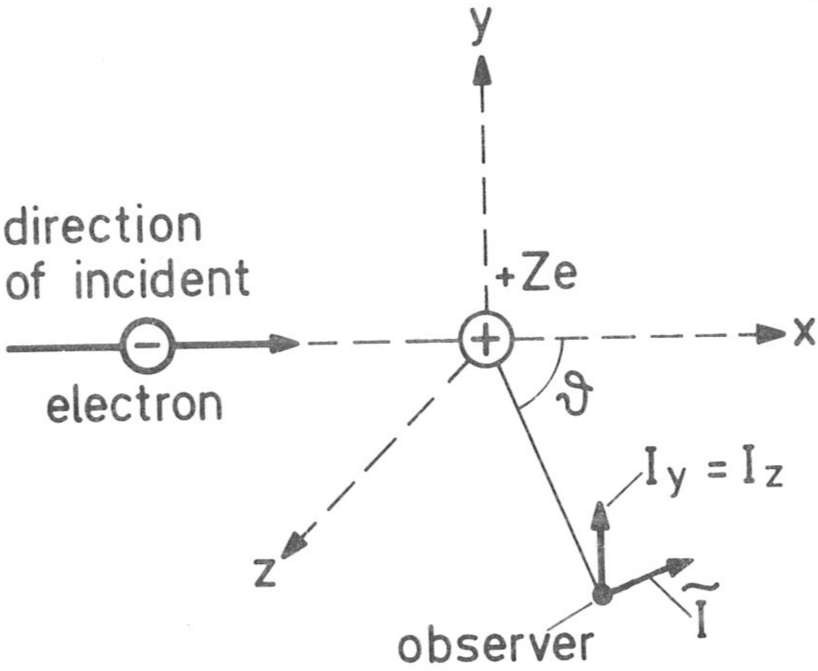

Fig.1 Definition of coordinates. Observer in the x-z plane. Polarization component I_y parallel to the y axis, $\tilde{I} = I_x \sin^2\vartheta + I_y \cos^2\vartheta$ perpendicular to the plane defined by the y axis and the line between the ion and observer

where

$$D = \frac{\pi}{2} \frac{Z^2 e^6 \xi_0^2}{c^3 m^2 v_1^2} \qquad \left(\xi_0^2 = - \frac{4 n_1 n_2}{(n_1 - n_2)^2} \right)$$

and

$$n_{1,2} = -i \frac{Z e^2}{\hbar v_{1,2}}$$

with i = imaginary unit and $m v_2^2/2 = E_1 - h\nu$.

$\mathfrak{M}_x^2$ and $\mathfrak{M}_y^2$ are given by the integrals

$$\mathfrak{M}_x^2 = - \frac{4\pi}{\xi_0} \left| \frac{2 n_1}{\xi_0} \right|^2 \int_0^{w_0} \left| \frac{n_1 + n_2}{n_1 - n_2} \cdot F(1 + n_1, -n_2, 1, w) - \frac{F(n_1, -n_2, 1, w)}{1 - w} \right|^2 dw \qquad (4a)$$

and

$$M_y^2 = \frac{8\pi}{\xi_0^3} |n_1(1+n_2)|^2 \cdot \int_0^{w_0} \left(\frac{\xi_0 w}{1-w} + \frac{w^2}{(1-w)^2} \right) \cdot |F(1+n_1-n_2, 2, w)|^2 dw \quad (4b)$$

where

$$w_0 = \frac{\xi_0}{\xi_0 - 1}$$

and F is the hypergeometric function defined by

$$F(a,b,c,x) = \sum_{\mu=0}^{\infty} g_\mu x^\mu$$

with $g_o = 1$ and $g_{\mu+1} = (\mu+a)(\mu+b)(\mu+1)^{-1}(\mu+c)^{-1} \cdot g_\mu$

These equations are used to evaluate the bremsstrahlung emission. Since they are only valid for a pure Coulomb potential, the results given below are restricted to plasmas with completely stripped ions and photon energies exceeding $\hbar\omega_p$; where $\omega_p = \left(\frac{ne^2}{m\varepsilon_0}\right)^{1/2}$ (n = electron density) is the plasma frequency. For the density of solid deuterium 5.9 x 10^{22} cm^{-3}, for example, one finds $\hbar\omega_p$ = 9 eV.

To evaluate the bremsstrahlung emission from eqs. (1 ... 4), the integrals eq. (4) must be calculated. As no analytical solution is known, I_x and I_y must be calculated numerically. This was done for $E_1/Z^2 \lesssim 1$ keV by Kirkpatrick /11/. As we are interested mainly in the free-free radiation of low Z plasmas, e.g. a deuterium plasma with Z = 1, we calculated $I_{x,y}$ for an extended energy region E_1/Z^2.

3. Results for a monoenergetic electron beam

Numerical results for a monoenergetic electron beam incident on an ion at rest according eqs.(1 ... 4) are presented in the table *). Besides I_x and I_y the intensity integrated over all solid angles

$$I_{tot} = \int I(\vartheta)\, d\Omega = \frac{8\pi}{3}(I_x + 2 I_y) \qquad (5)$$

is tabulated. The accuracy of the numerical calculation is better than 1 %. For a special case, incident electron energy E_1 = 2o keV, the dependence of I_x, I_y and I_{tot} on the photon energy $h\nu$ are shown in Fig.2. The total intensity I_{tot} decreases with increasing

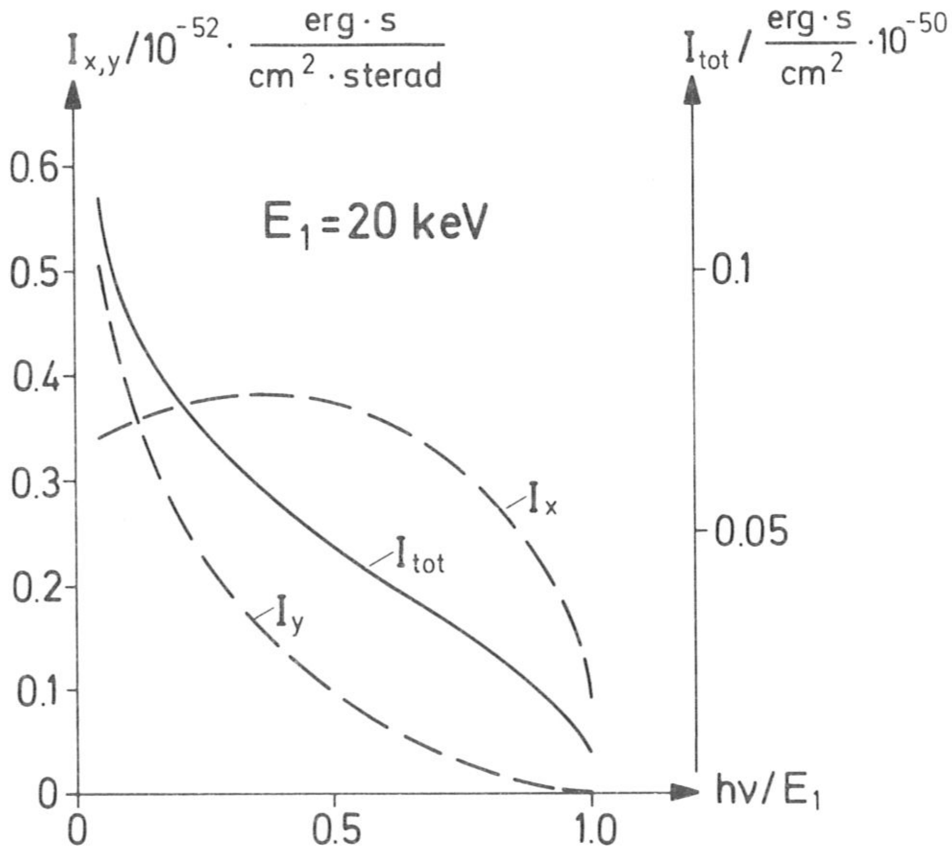

Fig.2 $I_{x,y}$ and I_{tot} as functions of $h\nu/E_1$ for E_1 = 2o keV

---

*) Here and in the following results Z = 1 was taken. The case Z > 1 can easily be found by replacing E_1 by E_1/Z^2 and $h\nu$ by $h\nu/Z^2$.

Table: Radiation components I_x, I_y and total intensity I_{tot} (in c.g.s units 10^{-50}) as a function of the photon energy $h\nu$ for different electron energies E_1.

E1/EV= 1.000E 03

HANY/EV	HANY/E1	IX	IY	ITOT
1.001E 01	1.001E-02	6.418E-02	1.492E-01	3.038E 00
5.000E 01	5.000E-02	6.826E-02	1.024E-01	2.288E 00
1.000E 02	1.000E-01	7.183E-02	7.926E-02	1.930E 00
1.500E 02	1.500E-01	7.453E-02	6.525E-02	1.718E 00
2.000E 02	2.000E-01	7.664E-02	5.509E-02	1.565E 00
2.500E 02	2.500E-01	7.828E-02	4.710E-02	1.445E 00
3.000E 02	3.000E-01	7.953E-02	4.051E-02	1.345E 00
3.500E 02	3.500E-01	8.044E-02	3.491E-02	1.259E 00
4.000E 02	4.000E-01	8.103E-02	3.005E-02	1.182E 00
4.500E 02	4.500E-01	8.130E-02	2.578E-02	1.113E 00
5.000E 02	5.000E-01	8.127E-02	2.200E-02	1.049E 00
5.500E 02	5.500E-01	8.095E-02	1.860E-02	9.898E-01
6.000E 02	6.000E-01	8.033E-02	1.556E-02	9.337E-01
6.500E 02	6.500E-01	7.939E-02	1.282E-02	8.799E-01
7.000E 02	7.000E-01	7.811E-02	1.035E-02	8.278E-01
7.500E 02	7.500E-01	7.648E-02	8.125E-03	7.768E-01
8.000E 02	8.000E-01	7.445E-02	6.129E-03	7.264E-01
8.500E 02	8.500E-01	7.198E-02	4.349E-03	6.759E-01
9.000E 02	9.000E-01	6.905E-02	2.781E-03	6.251E-01
9.500E 02	9.500E-01	6.582E-02	1.428E-03	5.754E-01
1.000E 03	1.000E 00	6.441E-02	2.851E-04	5.443E-01

E1/EV= 2.000E 03

HANY/EV	HANY/E1	IX	IY	ITOT
2.002E 01	1.001E-02	3.210E-02	7.473E-02	1.521E 00
1.000E 02	5.000E-02	3.407E-02	5.120E-02	1.143E 00
2.000E 02	1.000E-01	3.577E-02	3.952E-02	9.618E-01
3.000E 02	1.500E-01	3.703E-02	3.245E-02	8.539E-01
4.000E 02	2.000E-01	3.798E-02	2.732E-02	7.758E-01
5.000E 02	2.500E-01	3.869E-02	2.327E-02	7.140E-01
6.000E 02	3.000E-01	3.919E-02	1.994E-02	6.624E-01
7.000E 02	3.500E-01	3.950E-02	1.711E-02	6.176E-01
8.000E 02	4.000E-01	3.964E-02	1.466E-02	5.777E-01
9.000E 02	4.500E-01	3.960E-02	1.251E-02	5.414E-01
1.000E 03	5.000E-01	3.940E-02	1.061E-02	5.078E-01
1.100E 03	5.500E-01	3.902E-02	8.906E-03	4.761E-01
1.200E 03	6.000E-01	3.847E-02	7.390E-03	4.461E-01
1.300E 03	6.500E-01	3.773E-02	6.027E-03	4.171E-01
1.400E 03	7.000E-01	3.678E-02	4.805E-03	3.887E-01
1.500E 03	7.500E-01	3.560E-02	3.714E-03	3.605E-01
1.600E 03	8.000E-01	3.416E-02	2.743E-03	3.321E-01
1.700E 03	8.500E-01	3.238E-02	1.889E-03	3.029E-01
1.800E 03	9.000E-01	3.019E-02	1.152E-03	2.722E-01
1.900E 03	9.500E-01	2.746E-02	5.360E-04	2.391E-01
2.000E 03	1.000E 00	2.518E-02	5.647E-05	2.119E-01

E1/EV= 3.000E 03

HANY/EV	HANY/E1	IX	IY	ITOT
3.003E 01	1.001E-02	2.140E-02	4.984E-02	1.014E 00
1.500E 02	5.000E-02	2.269E-02	3.412E-02	7.617E-01
3.000E 02	1.000E-01	2.380E-02	2.631E-02	6.401E-01
4.500E 02	1.500E-01	2.461E-02	2.157E-02	5.676E-01
6.000E 02	2.000E-01	2.521E-02	1.813E-02	5.150E-01
7.500E 02	2.500E-01	2.564E-02	1.542E-02	4.732E-01
9.000E 02	3.000E-01	2.593E-02	1.319E-02	4.383E-01
1.050E 03	3.500E-01	2.610E-02	1.130E-02	4.080E-01
1.200E 03	4.000E-01	2.614E-02	9.660E-03	3.808E-01
1.350E 03	4.500E-01	2.606E-02	8.223E-03	3.561E-01
1.500E 03	5.000E-01	2.587E-02	6.952E-03	3.332E-01
1.650E 03	5.500E-01	2.555E-02	5.818E-03	3.115E-01
1.800E 03	6.000E-01	2.511E-02	4.809E-03	2.909E-01
1.950E 03	6.500E-01	2.453E-02	3.904E-03	2.709E-01
2.100E 03	7.000E-01	2.380E-02	3.095E-03	2.513E-01
2.250E 03	7.500E-01	2.291E-02	2.374E-03	2.317E-01
2.400E 03	8.000E-01	2.181E-02	1.737E-03	2.118E-01
2.550E 03	8.500E-01	2.046E-02	1.179E-03	1.912E-01
2.700E 03	9.000E-01	1.878E-02	7.029E-04	1.691E-01
2.850E 03	9.500E-01	1.660E-02	3.118E-04	1.443E-01
3.000E 03	1.000E 00	1.434E-02	2.153E-05	1.205E-01

E1/EV= 5.000E 03

HANY/EV	HANY/E1	IX	IY	ITOT
5.005E 01	1.001E-02	1.283E-02	2.989E-02	6.093E-01
2.500E 02	5.000E-02	1.360E-02	2.046E-02	4.567E-01
5.000E 02	1.000E-01	1.425E-02	1.576E-02	3.833E-01
7.500E 02	1.500E-01	1.471E-02	1.290E-02	3.394E-01
1.000E 03	2.000E-01	1.505E-02	1.083E-02	3.076E-01
1.250E 03	2.500E-01	1.529E-02	9.197E-03	2.822E-01
1.500E 03	3.000E-01	1.544E-02	7.853E-03	2.609E-01
1.750E 03	3.500E-01	1.551E-02	6.712E-03	2.424E-01
2.000E 03	4.000E-01	1.551E-02	5.726E-03	2.258E-01
2.250E 03	4.500E-01	1.542E-02	4.862E-03	2.107E-01
2.500E 03	5.000E-01	1.527E-02	4.098E-03	1.966E-01
2.750E 03	5.500E-01	1.504E-02	3.418E-03	1.833E-01
3.000E 03	6.000E-01	1.473E-02	2.814E-03	1.705E-01
3.250E 03	6.500E-01	1.433E-02	2.274E-03	1.582E-01
3.500E 03	7.000E-01	1.384E-02	1.792E-03	1.459E-01
3.750E 03	7.500E-01	1.323E-02	1.365E-03	1.337E-01
4.000E 03	8.000E-01	1.249E-02	9.881E-04	1.212E-01
4.250E 03	8.500E-01	1.159E-02	6.613E-04	1.081E-01
4.500E 03	9.000E-01	1.044E-02	3.848E-04	9.393E-02
4.750E 03	9.500E-01	8.918E-03	1.622E-04	7.743E-02
5.000E 03	1.000E 00	6.976E-03	6.303E-06	5.855E-02

E1/EV= 1.000E 04

HANY/EV	HANY/E1	IX	IY	ITOT
1.001E 02	1.001E-02	6.413E-03	1.496E-02	3.243E-01
5.000E 02	5.000E-02	6.791E-03	1.022E-02	2.292E-01
1.000E 03	1.000E-01	7.107E-03	7.863E-03	1.913E-01
1.500E 03	1.500E-01	7.331E-03	6.430E-03	1.692E-01
2.000E 03	2.000E-01	7.490E-03	5.389E-03	1.531E-01
2.500E 03	2.500E-01	7.597E-03	4.567E-03	1.402E-01
3.000E 03	3.000E-01	7.659E-03	3.894E-03	1.294E-01
3.500E 03	3.500E-01	7.680E-03	3.322E-03	1.200E-01
4.000E 03	4.000E-01	7.661E-03	2.827E-03	1.115E-01
4.500E 03	4.500E-01	7.602E-03	2.394E-03	1.038E-01
5.000E 03	5.000E-01	7.506E-03	2.012E-03	9.660E-02
5.500E 03	5.500E-01	7.369E-03	1.673E-03	8.976E-02
6.000E 03	6.000E-01	7.190E-03	1.371E-03	8.322E-02
6.500E 03	6.500E-01	6.965E-03	1.103E-03	7.683E-02
7.000E 03	7.000E-01	6.689E-03	8.637E-04	7.051E-02
7.500E 03	7.500E-01	6.353E-03	6.526E-04	6.416E-02
8.000E 03	8.000E-01	5.945E-03	4.677E-04	5.764E-02
8.500E 03	8.500E-01	5.442E-03	3.083E-04	5.076E-02
9.000E 03	9.000E-01	4.805E-03	1.750E-04	4.319E-02
9.500E 03	9.500E-01	3.937E-03	6.987E-05	3.416E-02
1.000E 04	1.000E 00	2.585E-03	1.171E-06	2.167E-02

E1/EV= 2.000E 04

HANY/EV	HANY/E1	IX	IY	ITOT
2.002E 02	1.001E-02	3.207E-03	7.475E-03	1.521E-01
1.000E 03	5.000E-02	3.393E-03	5.108E-03	1.140E-01
2.000E 03	1.000E-01	3.549E-03	3.926E-03	9.549E-02
3.000E 03	1.500E-01	3.656E-03	3.207E-03	8.437E-02
4.000E 03	2.000E-01	3.732E-03	2.685E-03	7.625E-02
5.000E 03	2.500E-01	3.781E-03	2.274E-03	6.977E-02
6.000E 03	3.000E-01	3.807E-03	1.935E-03	6.432E-02
7.000E 03	3.500E-01	3.812E-03	1.648E-03	5.955E-02
8.000E 03	4.000E-01	3.796E-03	1.401E-03	5.527E-02
9.000E 03	4.500E-01	3.761E-03	1.184E-03	5.134E-02
1.000E 04	5.000E-01	3.706E-03	9.929E-04	4.768E-02
1.100E 04	5.500E-01	3.630E-03	8.233E-04	4.420E-02
1.200E 04	6.000E-01	3.532E-03	6.730E-04	4.086E-02
1.300E 04	6.500E-01	3.410E-03	5.392E-04	3.760E-02
1.400E 04	7.000E-01	3.262E-03	4.205E-04	3.437E-02
1.500E 04	7.500E-01	3.082E-03	3.160E-04	3.111E-02
1.600E 04	8.000E-01	2.864E-03	2.247E-04	2.776E-02
1.700E 04	8.500E-01	2.596E-03	1.465E-04	2.420E-02
1.800E 04	9.000E-01	2.256E-03	8.166E-05	2.027E-02
1.900E 04	9.500E-01	1.788E-03	3.133E-05	1.550E-02
2.000E 04	1.000E 00	9.448E-04	2.143E-07	7.919E-03

E1/EV= 3.000E 04

HANY/EV	HANY/E1	IX	IY	ITOT
3.003E 02	1.001E-02	2.137E-03	4.982E-03	1.014E-01
1.500E 03	5.000E-02	2.261E-03	3.404E-03	7.597E-02
3.000E 03	1.000E-01	2.363E-03	2.615E-03	6.360E-02
4.500E 03	1.500E-01	2.434E-03	2.135E-03	5.617E-02
6.000E 03	2.000E-01	2.483E-03	1.787E-03	5.074E-02
7.500E 03	2.500E-01	2.515E-03	1.512E-03	4.640E-02
9.000E 03	3.000E-01	2.530E-03	1.286E-03	4.275E-02
1.050E 04	3.500E-01	2.532E-03	1.095E-03	3.956E-02
1.200E 04	4.000E-01	2.520E-03	9.297E-04	3.669E-02
1.350E 04	4.500E-01	2.495E-03	7.852E-04	3.405E-02
1.500E 04	5.000E-01	2.456E-03	6.579E-04	3.160E-02
1.650E 04	5.500E-01	2.403E-03	5.449E-04	2.926E-02
1.800E 04	6.000E-01	2.335E-03	4.449E-04	2.702E-02
1.950E 04	6.500E-01	2.251E-03	3.558E-04	2.482E-02
2.100E 04	7.000E-01	2.149E-03	2.770E-04	2.265E-02
2.250E 04	7.500E-01	2.026E-03	2.076E-04	2.045E-02
2.400E 04	8.000E-01	1.877E-03	1.471E-04	1.819E-02
2.550E 04	8.500E-01	1.693E-03	9.545E-05	1.579E-02
2.700E 04	9.000E-01	1.460E-03	5.276E-05	1.312E-02
2.850E 04	9.500E-01	1.139E-03	1.987E-05	9.874E-03
3.000E 04	1.000E 00	5.217E-04	7.888E-09	4.372E-03

E1/EV= 5.000E 04

HANY/EV	HANY/E1	IX	IY	ITOT
5.005E 02	1.001E-02	1.283E-03	2.989E-03	6.082E-02
2.500E 03	5.000E-02	1.356E-03	2.042E-03	4.558E-02
5.000E 03	1.000E-01	1.417E-03	1.568E-03	3.814E-02
7.500E 03	1.500E-01	1.459E-03	1.280E-03	3.367E-02
1.000E 04	2.000E-01	1.488E-03	1.070E-03	3.040E-02
1.250E 04	2.500E-01	1.506E-03	9.055E-04	2.779E-02
1.500E 04	3.000E-01	1.514E-03	7.698E-04	2.558E-02
1.750E 04	3.500E-01	1.514E-03	6.548E-04	2.366E-02
2.000E 04	4.000E-01	1.506E-03	5.556E-04	2.193E-02
2.250E 04	4.500E-01	1.490E-03	4.689E-04	2.034E-02
2.500E 04	5.000E-01	1.465E-03	3.924E-04	1.835E-02
2.750E 04	5.500E-01	1.432E-03	3.247E-04	1.744E-02
3.000E 04	6.000E-01	1.390E-03	2.647E-04	1.608E-02
3.250E 04	6.500E-01	1.338E-03	2.114E-04	1.475E-02
3.500E 04	7.000E-01	1.275E-03	1.642E-04	1.343E-02
3.750E 04	7.500E-01	1.199E-03	1.228E-04	1.210E-02
4.000E 04	8.000E-01	1.107E-03	8.671E-05	1.073E-02
4.250E 04	8.500E-01	9.941E-04	5.598E-05	9.266E-03
4.500E 04	9.000E-01	8.507E-04	3.068E-05	7.641E-03
4.750E 04	9.500E-01	6.524E-04	1.134E-05	5.655E-03
5.000E 04	1.000E 00	2.462E-04	2.236E-09	2.063E-03

$h\nu$ and reaches a finite minimum at the short wave limit $h\nu = E_1$. At the long wave limit $h\nu \rightarrow o$ I_{tot} becomes infinite owing to the fact that the Debey shielding is neglected.

From the given values of I_x and I_y the angular dependence of the intensity and the polarization can be calculated with the equations (1) and (2). An example for E_1 = 2o keV can be seen from Figs.3 and 4. $I(\vartheta)$ and $P(\vartheta)$ are symmetric with respect to ϑ = 9o°

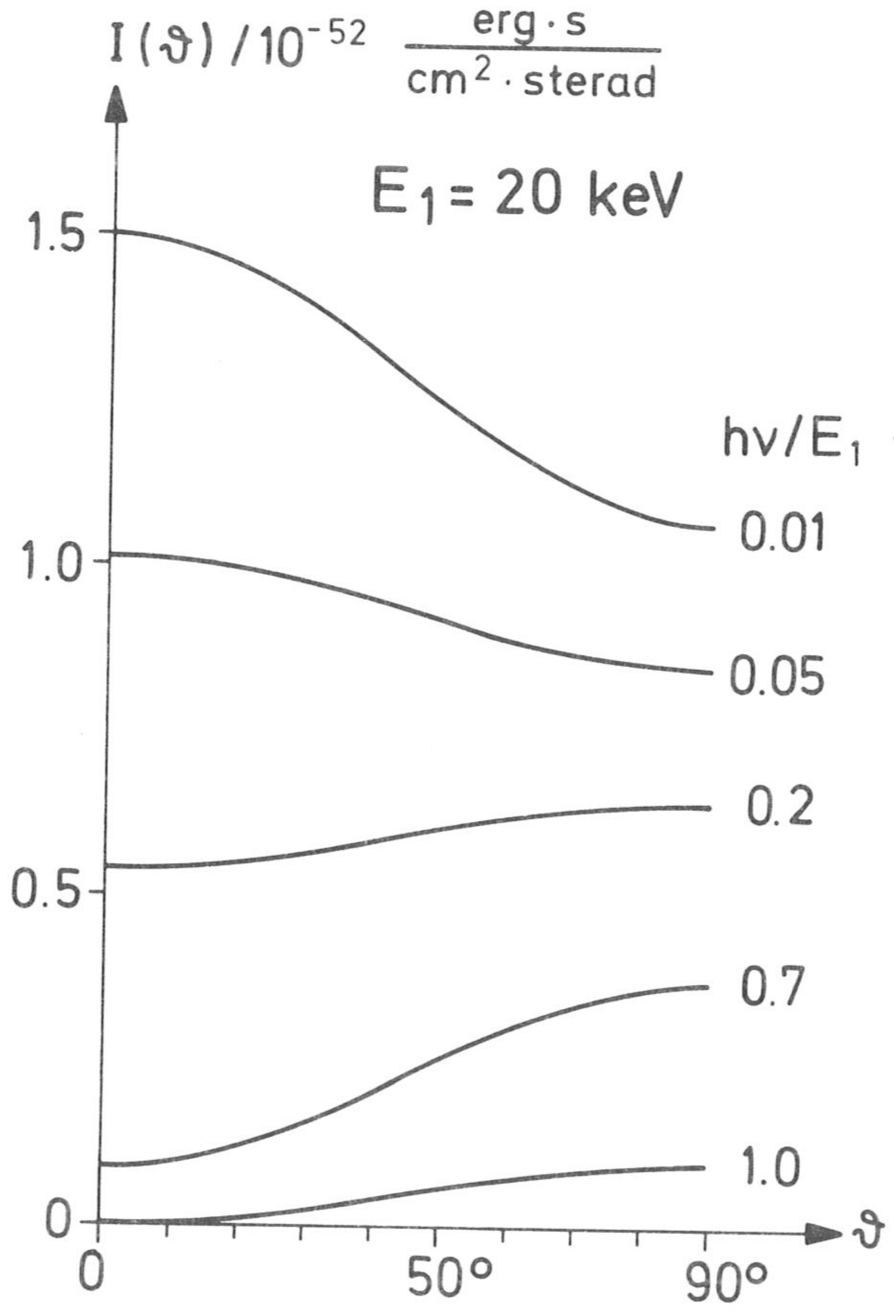

Fig.3 Angular dependence of intensity for some values of $h\nu/E_1$; E_1 = 1o keV

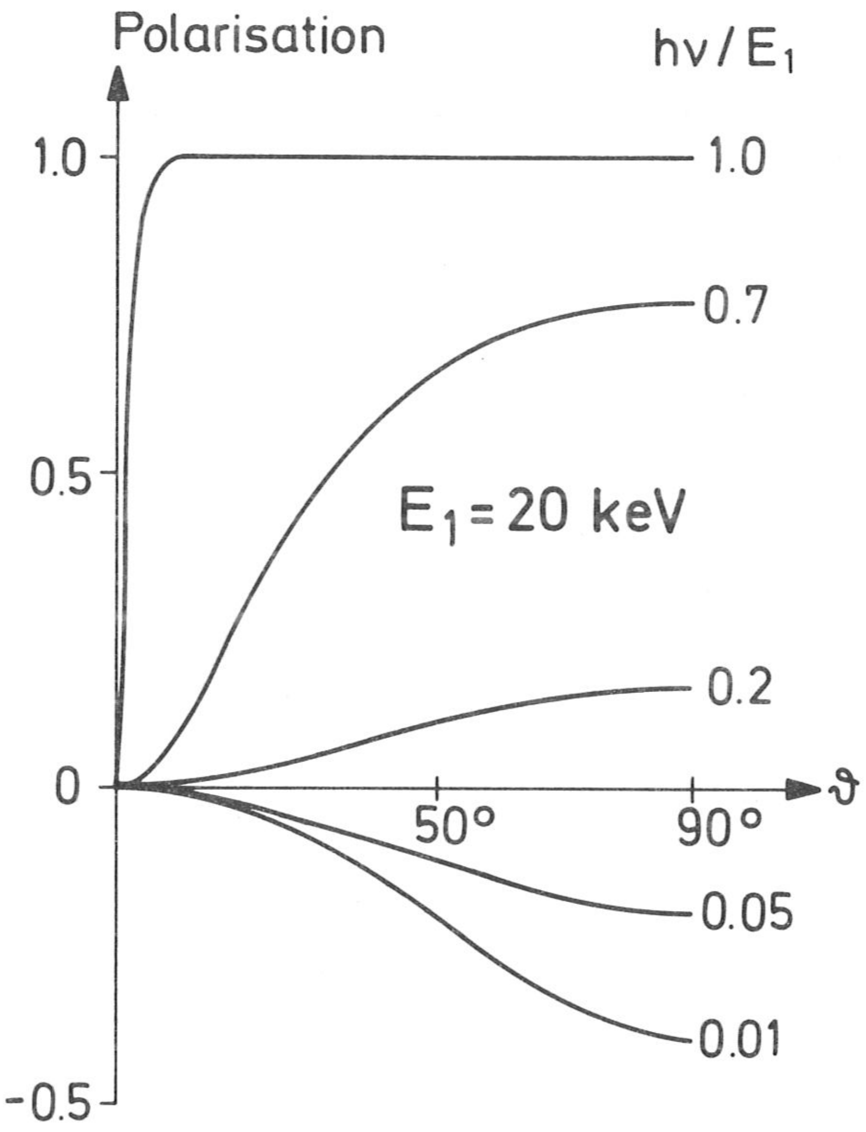

Fig.4 Angular dependence of the polarization for some values of h /E_1; E_1 = lo keV

since the calculations are restricted to the non-relativistic case. At the long wave limit the intensity has a maximum at ϑ = o^o , whereas at the short wave limit the maximum is at ϑ = 9o^o . The polarization for ϑ = o^o is equal to zero, which is clear for reasons of symmetry. For ϑ = 9o^o it is at the long wave limit perpendicular to the plane of the direction of observation and the axis of the incident electron current, i.e. parallel to the y-axis in fig.1; in the short wave limit it is parallel to the axis of the incident electron current (x-axis in fig.1). These results can be understood qualitatively in terms of classical electrodynamics if the electron accelerated in the electric field of the nucleus is considered as a radiating electric dipole, which is oriented in fig.1 at the short wave limit parallel to the x-axis, whereas at the long wave limit all directions of the dipole axis perpendicular to the x-axis are possible.

4. Isotropic electron velocity distribution

In a plasma with an electron velocity distribution $f(\vec{r}, \vec{v})$, where $\vec{r}$ is the position and $\vec{v}$ the electron velocity, the free-free radiation originating from an ion at position $\vec{r}$ is given by

$$g_{tot}(\vec{r}) = \int I(\vec{v})\, v\, f(\vec{r}, \vec{v})\, d^3\vec{v} \qquad (6)$$

where $vf(\vec{r},\vec{v})d^3\vec{v}$ is the electron current density of electrons with velocities within $\vec{v}$ and $\vec{v} + d\vec{v}$. The total intensity emitted from the plasma with ion density $n_i(\vec{r})$ can be calculated from

$$G_{tot} = \int n_i(\vec{r})\, g_{tot}(\vec{r})\, d^3\vec{r} \qquad (7)$$

assuming an optically thin plasma and plasma dimensions which are small relative to the distance of the observer from the plasma. For an isotropic velocity distribution one finds

$$g_{tot}(\vec{r}) = \int_{\sqrt{\frac{2}{m}h\nu}}^{\infty} I_{tot}\left(E_1 = \frac{m}{2}v^2, h\nu\right) v^3 f(\vec{r}, v)\, dv \qquad (8)$$

which is an integral over the velocity distribution $f(\vec{r}, v)$ weighted with the function I_{tot} $(E_1 = \frac{m}{2} v^2, h\nu)$ given by eq.(5). The typical dependence of I_{tot} on the incident electron energy $E_1 = \frac{m}{2} v^2$ is shown in fig.5 for $h\nu = 10$ keV.

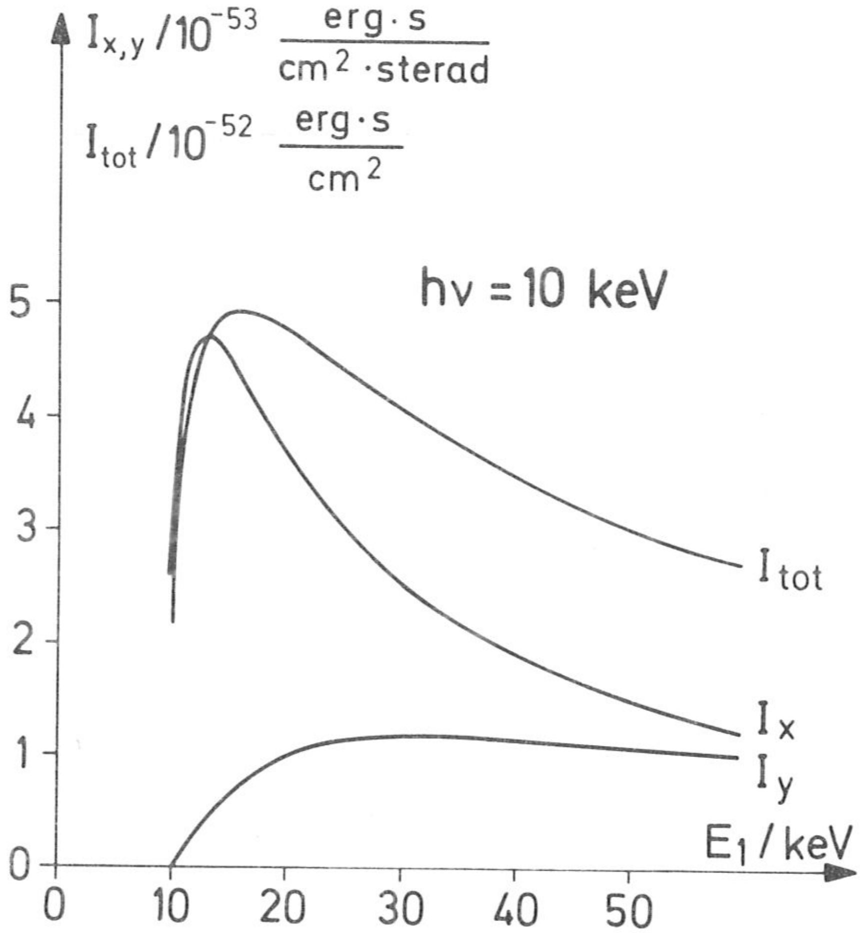

Fig.5 Dependences of I_x, I_y and I_{tot} on electron energy E_1 for a fixed photon energy h = 1o keV

As the exact shape of the electron velocity distribution is not known theoretically for laser produced plasmas, but an excess of fast electrons is typical, the bremsstrahlung was calculated from eq.(8) for some arbitrary spatially homogeneous distribution functions which show an excess of fast electrons. Some results for such non-Maxwellian distribution functions are given in figs. 6 ... 8. For comparison results for a purely Maxwellian distribution are shown in fig.9.

As the bremsstrahlung emitted from laser produced plasmas is observed in most cases by the absorbing foil method /12/, the quantity

$$S(E_c) = \int_0^\infty D(E_c, h\nu) \cdot g_{tot} \, d(h\nu) \qquad (9)$$

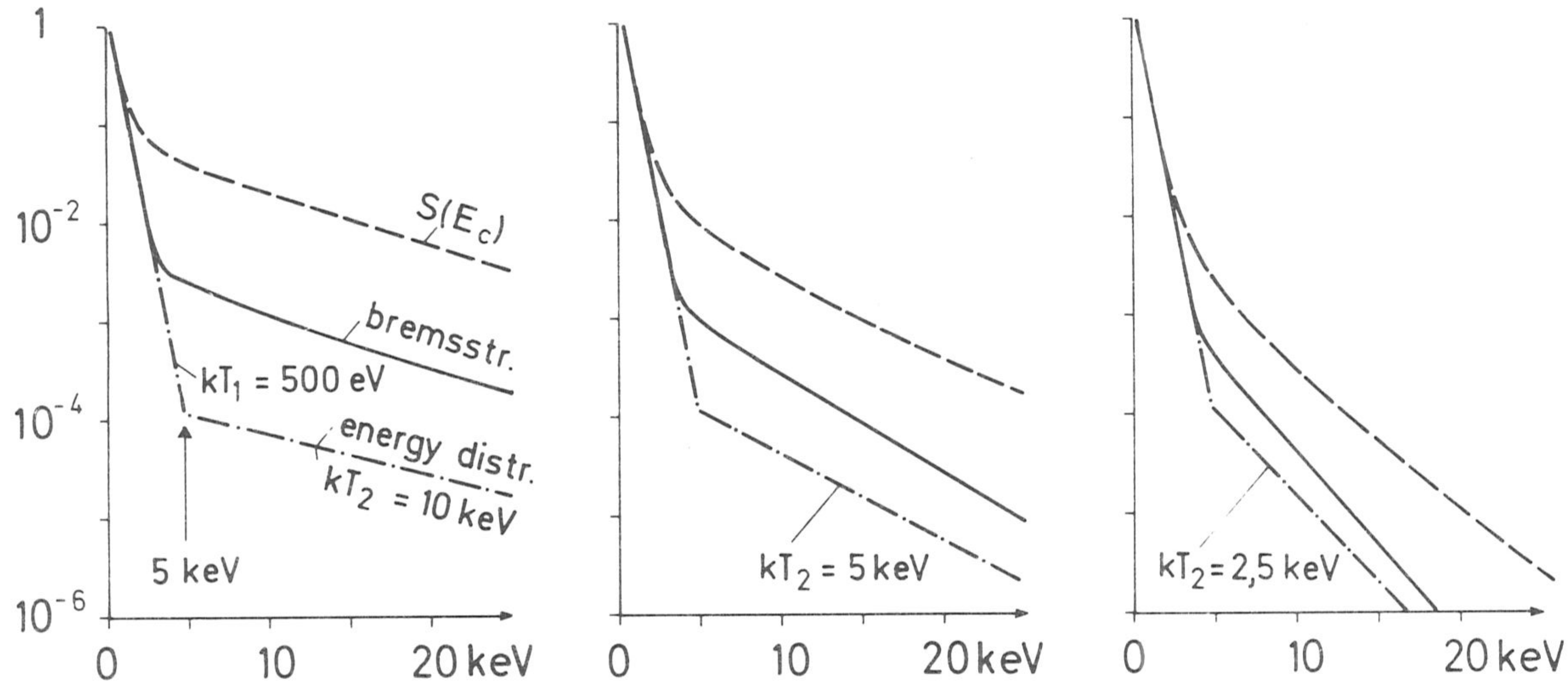

Fig.6 Normalized electron energy distribution function, bremsstrahlung spectrum and x-ray signal $S(E_c)$ transmitted through an absorbing foil of "cut-off energy" E_c as functions of electron energy $E = m/2\ v^2$, photon energy $h\nu$ and "cut-off energy" E_c respectively. Electron distribution function is $f(E) = \exp(-E/kT_1)$ for $E < 5$ keV and $f(E) \propto \exp(-E/kT_2)$ for $E > 5$ keV

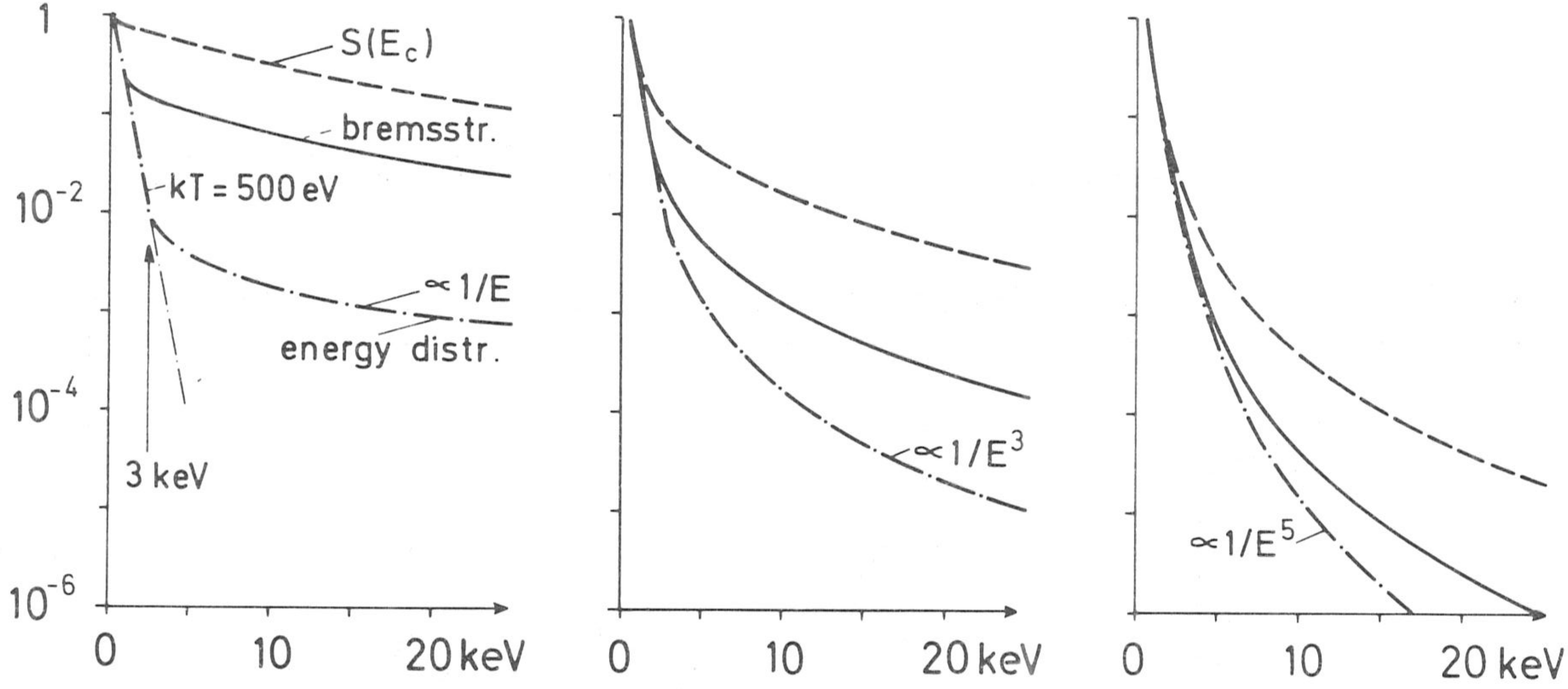

Fig.7 Like fig.6; example of an electron distribution function given by $f(E) = \exp(-E/kT)$, $kT = 500$ eV for $E < 3$ keV and $f(E) \propto E^{-\alpha}$ for $E > 3$ keV

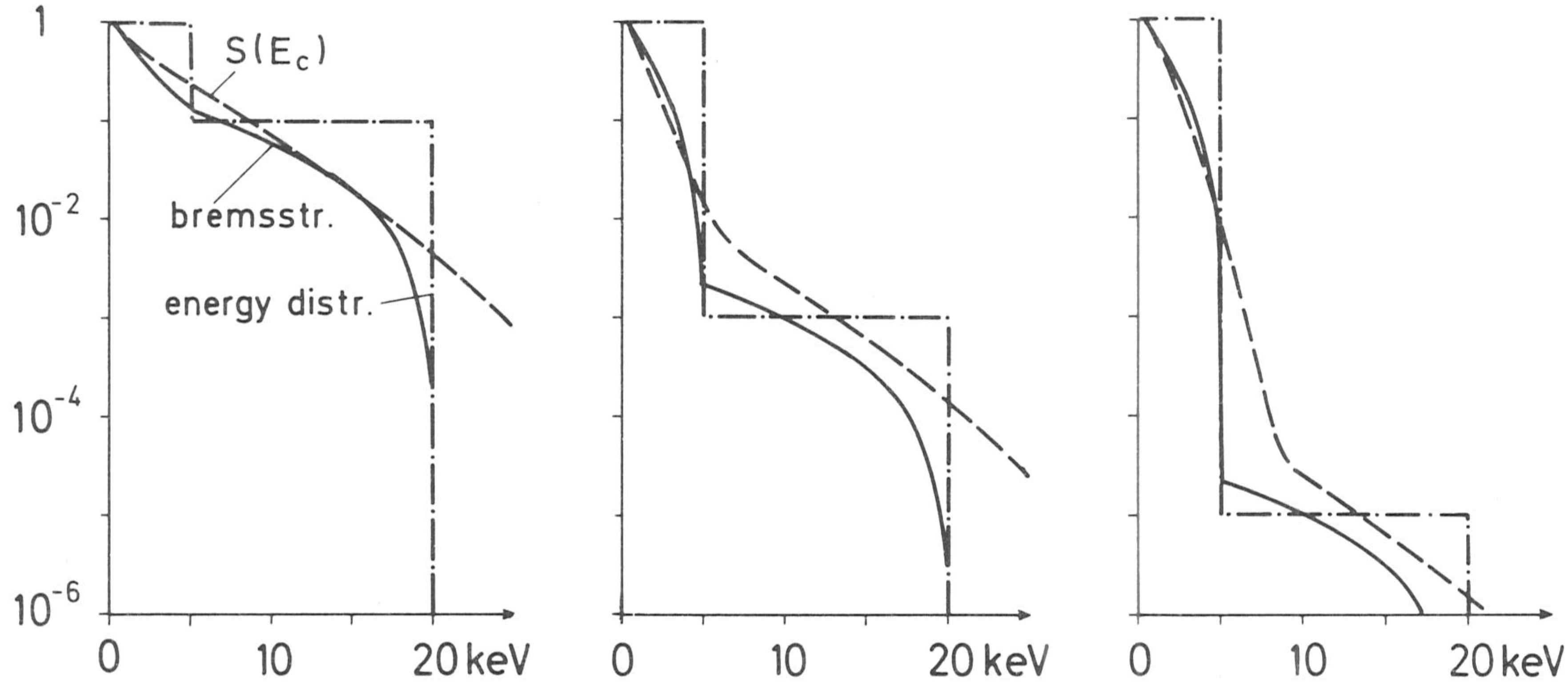

Fig.8 Like fig.6; example of an electron distribution function given by $f(E) = 1$ for $E < 5$ keV and $f(E) = const < 1$ for $E > 5$ keV

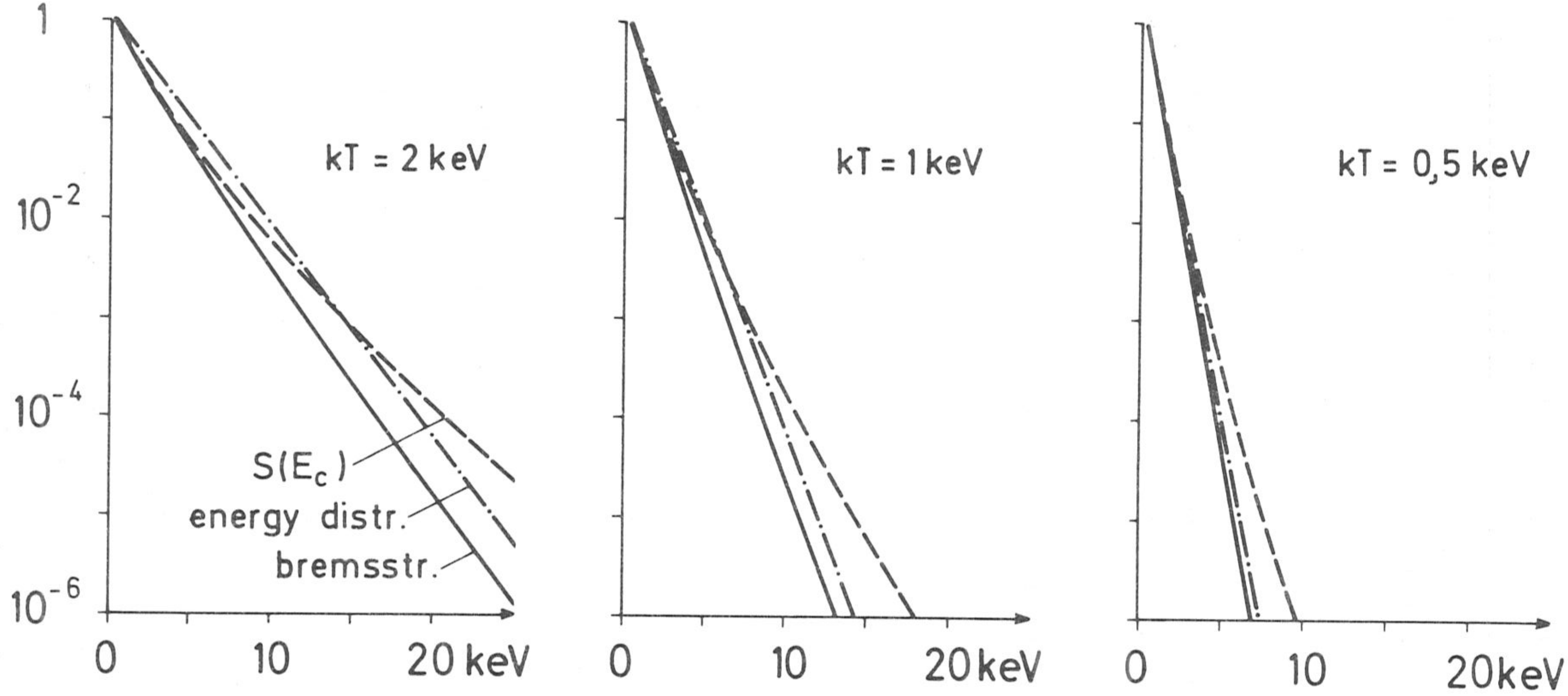

Fig.9 Like fig.6; Maxwellian distribution function

which is the amount of X radiation transmitted through the foil, was also calculated. $D(E_c, h\nu)$ is the foil transmittance for photons of energy $h\nu$, which in the calculations presented in figs. 7 ... 1o was expressed by the formula

$$D(E_c, h\nu) = \exp(-(E_c/h\nu)^{2,86})$$

This expression is valid in good approximation for Be and Al foils and photon energies above the K-edge /13/, which is 115 eV for Be and 1564 eV for Al. The cut-off energy E_c is related to the foil thickness by

$$(d/\mu m) = K(E_c/keV)^{2,86}$$

where K = 11 for Be and K = 2 for Al /13/.

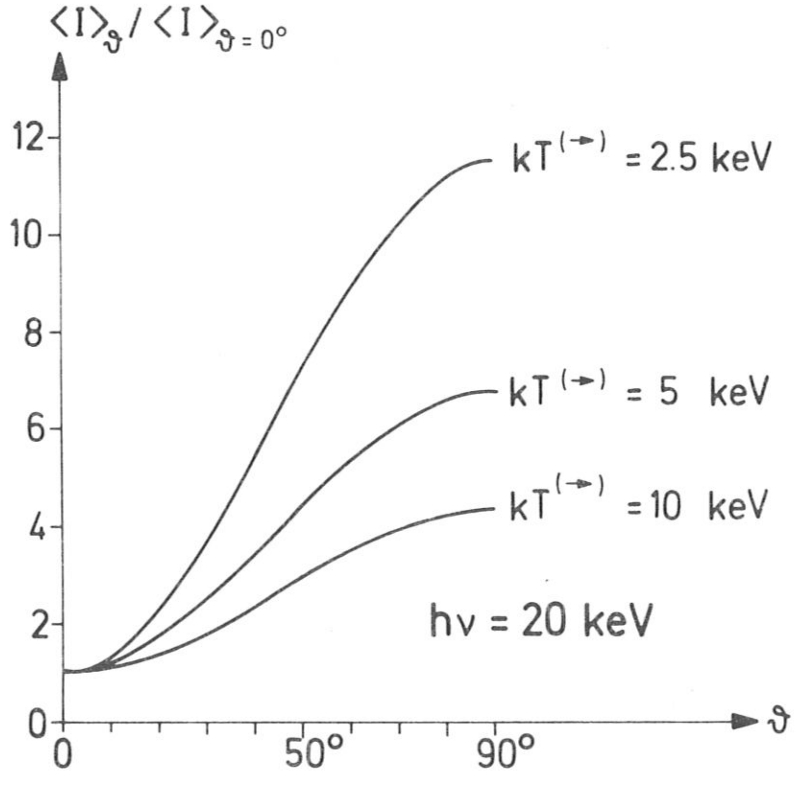

Fig.1o Dependence of the intensity on the angle ϑ between the direction of electron velocity and the direction of observation for different "directed temperatures" $kT^{(\rightarrow)}$

For a Maxwellian distribution (see fig.9) the bremsstrahlung and $S(E_c)$ show in good approximation an exponential dependence on the photon energy $h\nu$ and cut-off energy E_c respectively. This is not so for the non-Maxwellian cases in figs. 6 ... 8, which demonstrate well that an excess of fast electrons may be detected in the bremsstrahlung spectrum as well as in the signal $S(E_c)$ transmitted through the absorbing foil. However, comparison of the results in figs. 6 ... 8 shows that the exact structure of the distribution function is smeared out by the bremsstrahlung spectrum, which according to eq.(8) is approximately an integral over the distribution function for electron energies exceeding $h\nu$, and still more by the function $S(E_c)$, which according to eq.(8) is an integral over the bremsstrahlungs spectrum and hence roughly a two-fold integral over the distribution function.

5. Anisotropic velocity distribution

In the case of anisotropic electron velocity distribution the plasma emits anisotropic bremsstrahlung. As can be seen from figs. 3 and 4, the bremsstrahlung is radiated for a monoenergetic electron beam at the short wave limit with a large intensity anisotropy and a polarization of almost 1oo %. However, if electrons of different energies E_1 are present, it is possible at a fixed photon energy $h\nu$ to have contributions from the short wave limit $E_1 = h\nu$ as well from electrons with energies $E_1 > h\nu$. As the behaviour of the x-ray anisotropy at the short wave limit and at the long wave limit is quite opposite according to figs.3 and 4, the dominating contribution has to be determined by integrating over the electron velocities.

For simplicity we consider the ideal case where the electrons are completely directed as represented by a one-dimensional distribution function $f_1(v_x)$. This is justified if it is assumed that a strong electric field directed parallel to the x-axis accelerates the electrons to high energies, as is possible in laser produced plasmas owing to, for example, resonant absorption /4/. If in addition electrons with isotropic velocities are present, the total x-ray emission can easily be found by combining the results of this and the previous section.

For a spatially homogeneous plasma the angular dependence of the intensity and polarization due to f_1 is given by

$$\begin{aligned}\langle I \rangle &= \int_{-\infty}^{+\infty} I(\vartheta)\, v_x f_1(v_x)\, dv_x \\ &= g_x \sin^2\vartheta + g_y (1+\cos^2\vartheta)\end{aligned} \tag{1o}$$

and

$$\langle P \rangle = (g_x - g_y) \Big/ \left(g_x + g_y \frac{\cos^2\vartheta + 1}{\sin^2\vartheta} \right) \tag{11}$$

with

$$g_{x,y} = \int_{-\infty}^{+\infty} I_{x,y}\left(\frac{m}{2} v_x^2, h\nu\right) v_x f_1(v_x)\, dv_x \tag{12}$$

and ϑ the angle between v_x and the direction of observation.

For $h\nu$ = lo keV the dependence of I_x and I_y is shown in fig.7. Since I_x and I_y are not strongly peaked at $E_1 = h\nu$, the values of the integrals depend on the special structure of the electron distribution function $f(v_x)$. The integration of eq.(12) was performed for a directed high energy tail of the form

$$f_1(v_x) \propto \exp\left(-\frac{m}{2} v_x^2 / kT^{(\rightarrow)}\right)$$

for different "directed temperatures" $T^{(\rightarrow)}$. Results are given in figs. lo ... 13. Figures lo and 11 show the angular dependence of the intensity and polarization respectively for different $kT^{(\rightarrow)}$. The maximum intensity anisotropy as well as the maximum polarization

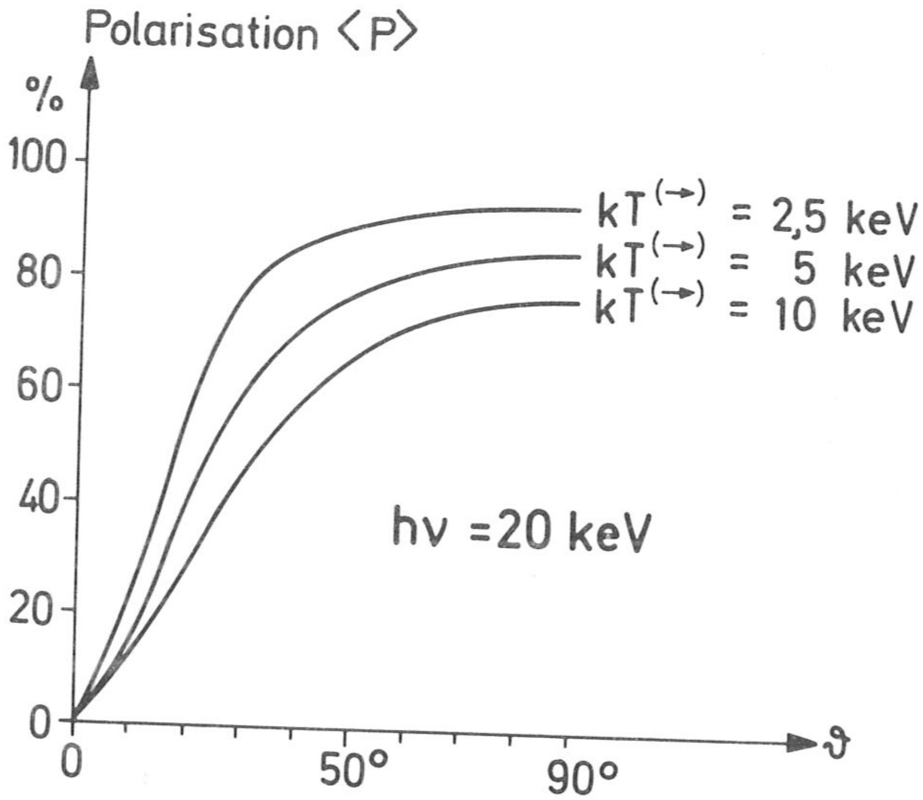

Fig.11 Dependence of the polarization on ϑ for different $kT^{(\rightarrow)}$

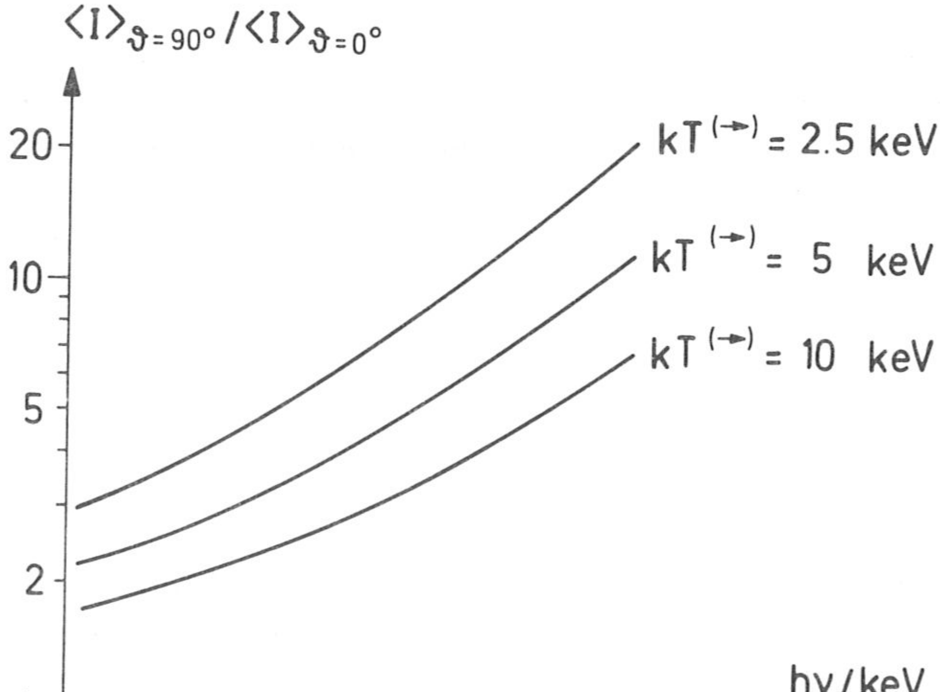

Fig.12 Intensity anisotropy as a function of $h\nu$ for different $kT^{(\rightarrow)}$

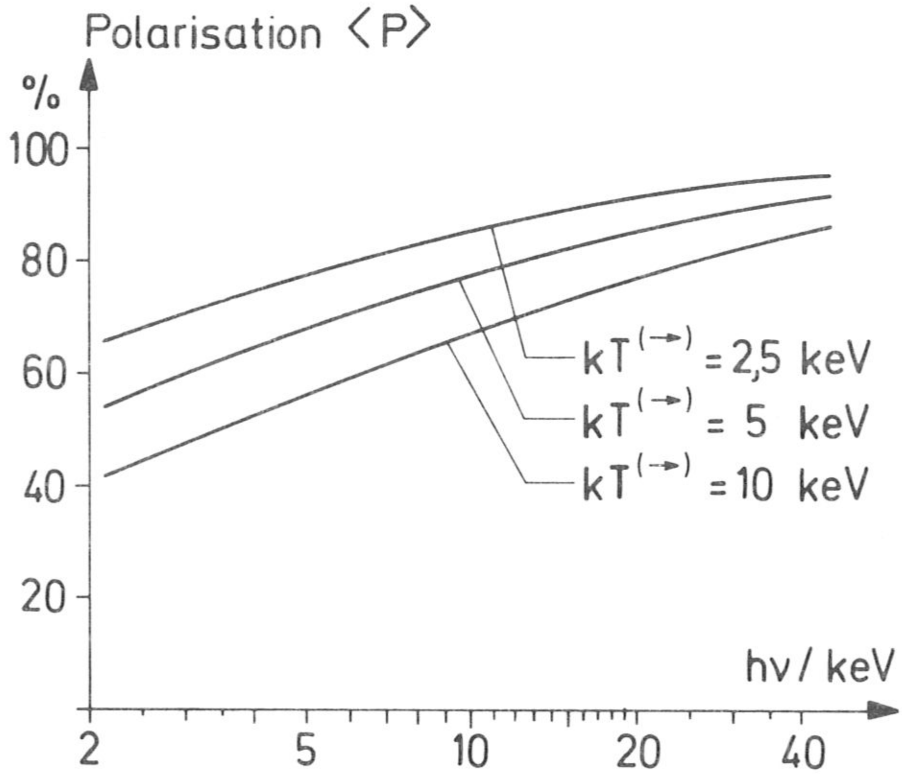

Fig.13 Polarization as a function of h for different kT( )

are obtained for ϑ = 9o $^{\circ}$ here. The dependence of these quantities on the photon energy $h\nu$ are shown in figs.12 and 13. The results show that the contribution from the short wave limit and hence the anisotropy of the emitted x-rays increases with increasing photon energy and decreasing slope of the distribution function.

5. Conclusions

In this study the properties of the free-free radiation due to electron ion collisions from a plasma with non-Maxwellian velocity distributions were investigated. The x-ray emission was calculated on the assumption of non-relativistic electron energies, pure Coulomb potential of the ions in the plasma, which is assumed to be optically thin to the x-ray energies considered. The results show that an excess of fast electrons can easily be observed in the x-ray emission. However, the bremsstrahlung spectrum is not very sensitive to the particular shape of the electron distribution function. Thus, if the electron distribution function is to be calculated from the bremsstrahlung spectrum, very accurate measurements are necessary.

Calculations for the case of anisotropic electron distribution functions which decrease with increasing electron energy show that anisotropy of the distribution function can readily be detected by measuring the angular dependence of either the polarization or the intensity. An increasing x-ray anisotropy can be observed with increasing photon energy.

To calculate the space integrated x-ray emission from inhomogeneous plasmas, the spatial variation of the electron velocity distribution and of the ion density must be known (see eq.7). In laser produced plasmas strong inhomogeneous situations are possible. The fast electrons can be generated in a region of relative low density, where the plasma frequency equals the laser frequency /4/. They may then move into a region of higher density, in which the x-rays are mainly emitted. The study of this problem was beyond the aim of this paper. However, the results presented here can be directly applied if spatially homogeneous parts of the plasma are observed.

References

1 W.J. Karzas, R. Latter, Astrophys. J., Suppl. (1961) 167

2 P. Mulser, R. Sigel, S. Witkowski, Phys. Reports 6C (1973) 187

3 J. Nuckolls, L. Wood, A. Thiessen, G. Zimmermann, Nature 239 (1972) 139

4 W.L. Kruer, J.M. Dawson, Phys. Fluids 15 (1972) 446; D.W. Forslund, J.M. Kindel, E.L. Lindman, Phys. Rev. Lett. 29 (1973) 249; J.P. Friedberg, R.W. Mitchell, R.L. Morse, L.T. Rudsinski, Phys. Rev. Lett. 28 (1972) 795

5 R. Sigel, S. Witkowski, H. Baumhacker, K. Büchl, K. Eidmann, H. Hora, H. Mennicke, P. Mulser, D. Pfirsch, H. Salzmann, IPP Report IV/9, Jan. 1971 and Quantovaya Elektronika 2 (1972) 37; J. W. Shearer, S.W. Mead, J. Petruzzi, F. Rainer, J.E. Swain, C.E. Violet, Phys. Rev. A6 (1972) 764; J.F. Kephart, R.P. Godwin, G.H. McCall, Bull. APS (1972) 971

6 K. Eidmann, R. Sigel, 6. European Conference on Controlled Fusion and Plasma Physics, Moscow, 3o.7. - 4.8.1973, Vol. 1, Contributed Papers, p. 435

7 R.P. Godwin, J.F. Kephart, G.H. McCall, Bull. APS (1972) 971

8 J.L. Shohet, Phys. Fluids 11 (1967) 1o65; P.A. Raimbault, J.L. Shohet, Phys. Fluids 15 (1972) 1477

9 A. Sommerfeld, Ann. d. Phys. 11 (1931) 257

1o R. Weinstock, Phys. Rev. 61 (1942) 584

11 P. Kirkpatrick, L. Wiedmann, Phys. Rev. 67 (1945) 321

12 F.C. Jahoda, E.M. Little, W.E. Quinn, G. A. Sawyer, T.F. Stratton, Phys. Rev. 119 (196o) 843

13 F.R. Gilmore, Research Memorandum RM-2367-AEC, Apr. 1959